UNSTEADY SEPARATION IN TWO-DIMENSIONAL TURBULENT FLOWS

Dipl.-Ing. H. Ranke,
Scientific Assistant,
Lehrstuhl für Fluidmechanik[1], Technische Universität München,
D-80290 München,
Germany

Abstract

Unsteady separation is still a subject of fundamental fluid mechanics which is not yet fully understood. In contrary to steady two-dimensional separation, where after Prandtl a semi bubble occurs, unsteady separation can be associated whith a full bubble within the boundary layer.

In a recent report[1] by the author and B. Laschka, which is in the process of beeing published, new light has been shed on the phenomenon of two-dimensional laminar separation in unsteady flow. There it could be shown that the familiar Moore-Rott-Sears criterion (MRS) is not sufficient to describe unsteady separation properly. It states that the onset of separation is reached if in a coordinate system moving with the separation point both the velocity parallel to the wall as well as its normal derivative vanish at one point simultaneously. This is however not a complete description.

It has been shown that the up–to–now description for relative to a fixed wall upstream moving separation point is in principle correct, but should be refined. It is, however, not correct for a downstream moving separation point. A new solution has been suggested there. The paper extends ref.1 to turbulent boundary layers, in particular.

Furtheron this new pattern are used for the interpretation of unsteady flowfield measurements at a pitching airfoil in dynamic stall motion. These results obtained with a new developed four-wire probe deal among other things with the onset of the Dynamic Stall Vortex and the reattachement, which are unsteady boundary layer effects.

Nomenclature

Symbols:

a, b	constants of WJ flow or geometry (swinging arm calibration)
$E_1 - E_3$	hot-wire voltages
f	frequency
k	reduced frequency, $k = fl_\mu/U_0$
L	characteristic length
l_μ	wing mean aerodynamic chord
p	static pressure
p_e	external flow static pressure
Re	Reynolds number, $Re = U_0 L/\nu$
Re_T	turbulence Reynolds number, $Re_T = U_0 L/\nu_T$
T	time of one pitching cycle
t	time
U_e	external flow velocity
U_0	reference velocity
u, v	flow components in x- and y-direction
u_1, v_1	velocities at the end of the computational area
u_w, v_w	wall velocities
w	total velocity, $w = sgn(u) * \sqrt{u^2 + v^2}$
x, y	wall fixed coordinate system
α	angle of attack
δ	boundary layer thickness
η	transformed coordinate y
ν	kinematic viscosity
ν_T	eddy viscosity
θ	phase angle (swinging arm calibration)

Abbreviations:

BL	Baldwin Lomax
CS	Cebeci Smith
MRS	Moore-Rott-Sears
ORF	Onset of Reverse Flow
STG	Stagnation
WJ	Williams-Johnson

Superscripts:

$\bar{}$	transformed coordinates and flow components

Introduction

It is well known that under unsteady flow conditions the boundary layer velocity profiles and the separation process is different from that under steady conditions. In ref.2 B. Laschka has compared unsteady and quasisteady boundary layer profiles of a quasi-Howarth flow which is retarded streamwise and in time, furtheron called Williams-Johnson (WJ) flow[3]. It is remarkable, that the velocity profiles at equal times show large differences. The quasisteady layers are much thinner than the unsteady ones, they show separation at other times and there is no way to predict the unsteady flow pattern by quasisteady means in an approximate way cor-

[1] Director: Prof. Dr.-Ing. B. Laschka

rectly. Fig. 1b compares the u-velocity profiles close to separation for a steady, a quasisteady and an unsteady approach of a WJ flow with a given external velocity, see Fig. 1a.

Steady two-dimensional separation is characterized by a semi-bubble. Its region is limited by the wall and by the separation line. At unsteady flow separation instead full bubbles, limited by the streamlines which belong to a free stagnation point, can be observed. Reverse flow components without any indication of separation are possible.

It is therefore not correct to describe the onset of unsteady separation according to the classical definition after L. Prandtl via vanishing skin friction ($\delta u/\delta y = 0$ at $y = 0$). Therefore F. K. Moore[4], N. Rott[5] and W. R. Sears[6] proposed independently of each other at the end of the fifties the so called MRS point as the onset of unsteady separation. The MRS criterion says that in a coordinate system moving with the separation point the velocity component along the wall direction and its normal derivative ($u = 0; \delta u/\delta y = 0$) vanish simultaneously in one point of the flow field. Streamline pictures, achieved e.g. from experiments of G. R. Ludwig[7] and of C. A. Koromilas and D. P. Telionis[8] seem to confirm that hypothesis, but there are some details which are not completely accounted for by the MRS criterion. In a recent report[1] those details are discussed consequently leading to a more refined description for unsteady separation. In the present paper the calculations are extended to turbulent flows leading to the result that the qualitative flow pattern is nearly unchanged.

The basis of this investigation is a qualitative analysis of the streamline pictures in a wall fixed or moving coordinate system, respectively. If the separation point only is wanted, there exist surely more accurate methods, e.g. that of L.L. van Dommelen[9]. In this paper, however, the author concentrate to obtain and analyze the flow pattern. This is important for a better understanding of the process of unsteady separation and for the possibility to interpret unsteady flow field measurements.

The second part of this paper deals with those unsteady flowfield measurements at a NACA 0012 airfoil in dynamic stall motion. It is well known that the separation process at pitching airfoils is different from that of a steady case[10, 11]. Fig. 2 compares a smoke visualisation of a steady and of a unsteady flow around a airfoil at same angle of attack.

The probe used for the dynamic stall study is a newly developed cross-wire probe with two additional wires to measure both streamwise and reverse flow. The results of this investigation show apart from other observations that the onset of the dynamic stall vortex and the reattachment are boundary layer driven effects. This agrees well with the proposed description of the phenomenon of unsteady separation.

Fundamentals

Basic Equations, Numerical Codes And Turbulence Model

The first order boundary layer equations for two-dimensional, incompressible, laminar, unsteady flows (see e.g.: H. Schlichting[12]) are as follows:

$$\frac{\partial u}{\partial x} + \frac{\partial v}{\partial y} = 0 \tag{1}$$

$$\frac{\partial u}{\partial t} + u\frac{\partial u}{\partial x} + v\frac{\partial u}{\partial y} = -\frac{\partial p_e}{\partial x} + \frac{1}{Re}\frac{\partial^2 u}{\partial y^2} \tag{2}$$

$$\frac{\partial p}{\partial y} = 0 \tag{3}$$

Boundary conditions:

$$\begin{aligned} &At\ y = 0 \ : \ u = u_w; \ v = v_w \\ &At\ y = \delta \ : \ u = U_e; \ \frac{\partial u}{\partial y} = 0 \\ &\Rightarrow \quad -\frac{\partial p_e}{\partial x} = \frac{\partial U_e}{\partial t} + U_e\frac{\partial U_e}{\partial x} \end{aligned} \tag{4}$$

For the turbulent calculations the eddy viscosity ($Re_T = U_0 L/\nu_T$) has to be added in Eqs. (2), see e.g. A.D. Young[13]:

$$\frac{1}{Re}\left(\frac{\partial^2 u}{\partial y^2}\right) \rightarrow \left(\frac{1}{Re} + \frac{1}{Re_T}\right)\left(\frac{\partial^2 u}{\partial y^2}\right) + \frac{\partial(1/Re_T)}{\partial y}\frac{\partial u}{\partial y} \tag{5}$$

A two layer zero equation model is used to achieve Re_T. For the inner layer the model of Cebeci and Smith (CS)[14, 15] is used. For the outer layer the model of Baldwin and Lomax (BL)[16, 17] was extended by the unsteady terms of the CS model. Results achieved with this model agree well with results from the literature for moderate pressure gradients and are sufficient for the mostly qualitative results in this paper.

The method used here to solve these equations (Eqs. (1-6)) is a time marching implicit code. For that purpose the boundary layer equations have been modified by adding the diffusive term $\partial^2 u/\partial x^2$ which occurs in the full Navier–Stokes equations. It balances the pressure gradient term in the momentum equation in regions of the flow field, where u and $\partial u/\partial y$ become very small, see D. T. Tsahalis[18]. It enables the calculation of flows with small regions of reverse flow or with small separation bubbles. The code used here is not very refined and there exist better ones, but it is sufficient for our purpose.

Williams-Johnson Flow

Certain classes of two-dimensional flows can be transformed such that the unsteady flow field quantities $f(x,y,t)$ become steady $f(\overline{x},\overline{y})$. These so-called semisimilar solutions[19, 3] are e.g. the Tani flow, the Curle Cubic flow, the Howarth linearly retarded flow and the WJ flow, which has been mentioned already before. This WJ flow[3] where an unsteady locally and temporarily linear retarded flow is transformed into a steady flow over a moving wall, is used in this paper partially in a modified form. A comparison of the results calculated for the retarded flow as well as for the equivalent form over a moving wall enables an easier understanding of the phenomenon of boundary layer separation for laminar as well as for turbulent flows.

The velocity of the external flow and the boundary conditions are as follows:

$$U_e = U_0(1 - Ax - Bt) \tag{6}$$

$$u = 0 \quad for \quad y = 0; \quad u = U_e \quad for \quad y = \delta$$

The transformation

$$x = \overline{x} + \int_{t_0}^{t} U dt; \quad y = \overline{y}; \quad t = \overline{t}$$

$$u = \overline{u} + U; \quad U = -\frac{B}{A}U_0; \quad v = \overline{v} \tag{7}$$

applied to equ. (6) yields to the time independent form:

$$\overline{U}_e = \overline{U}_0(1 - A\frac{1}{1 + B/A}\overline{x}); \quad \overline{U}_0 = U_0(1 + \frac{B}{A}) \tag{8}$$

$$\overline{y} = 0 \Rightarrow \overline{u} = -\frac{U}{\overline{U}_0}U_0; \quad \overline{y} = \delta \Rightarrow \overline{u} = \overline{U}_e$$

A more detailed description of this kind of flow is given by Williams and Johnson[3].

The original WJ flow and, in addition, a modified form which allows the calculation of a small separation bubble were evaluated. Both cases, namely the flows over an upstream and over a downstream moving wall will be considered. Those flows correspond to downstream and upstream moving separation points, respectively. Table 1. gives a short overview about the calculations done.

Upstream Moving Separation Point

Velocity Profiles In x- And y-Direction:

Fig. 3a shows the profiles of the u-component of the laminar WJ flow (see Tab. 1) normal to the wall, i.e. vs. $\eta = y * \sqrt{Re}$. This figure as well as those published by other authors, like D. P. Telionis and M. J. Werle[20], which holds for a wall velocity of $0.06 * U_e$, and others[21, 22, 3, 19] reveal that there are no intersections of the velocity profiles upstream of the MRS point neither for the steady calculations in the separation point fixed nor for the unsteady calculations in the wall fixed coordinate system. As a consequence in front of the MRS point the flow component u is decelerated at any distance from the wall. This holds for laminar as well as for turbulent flows, only the profiles are thicker in the turbulent case. Fig. 3b shows the velocity profiles immediately before separation is reached for a laminar and a turbulent WJ flow.

As the u-component decreases at any distance from the wall before separation is reached, the v-component is always upward (positive) directed upstream of the MRS point. This is in accordance with the continuity equation. When the flow approaches the MRS point v becomes very large. Because of the simplifications which underlie the boundary layer equations the calculation shows even a singularity. Fig. 4a shows the strong increasing of the displacement thickness near the separation. The wall shear stress, Fig. 4b passes the zero line without any sign of instability.

Streamline Pictures

Fig. 5a is a typical reproduction of streamlines in the separation point fixed coordinate system, e.g. taken from D. P. Telionis and M. J. Werle[20]. In this picture or in similar pictures e.g. those by C. A. Koromilas and D. P. Telionis[6] or G. R. Ludwig[23], there are some inaccuracies in the details which account neither for the physics nor for the basic equations. This is explained by the following deliberations using the abbreviations ORF for Onset of Reverse Flow and STG for Stagnation. We now follow the arguments of ref.1:

1. **At the MRS-point the streamline must be perpendicular to the wall:** When the flow is approaching the MRS point the u-component becomes zero whereas the v-component becomes very large in order to be consistent with the continuity equation. A finite slope of the MRS-streamline would otherwise require a negative u-component upstream of the MRS point.
2. **The MRS point and the STG point cannot coincide:** At the MRS point only the u-component is zero, the v-component is positive. At the STG point, however, both velocity components do vanish.

Chapter	Kind of Separation	Calculation (grid: 91*91)	u_e; u_w; x_1; Re	Fig.
3	downstream moving wall equiv. to upstream moving separation laminar and turbulent case	steady, WJ flow	$u_e = 1 - 0.833x$ $u_w = 0.166$ $Re = 10^6$ $x_{1,l} = 0.314$ $x_{1,t} = 0.636$	3,4
3	upstream moving separation equiv. to downstream moving wall turbulent case	unsteady, modified WJ flow	$u_e = 1 - x - 0.2t$ $x < x_I$ $u_e = 1 - x_I - 0.2t$ $x > x_I$ $x_I = 0.945x_1$ $x_1 = 0.05$ $Re = 10^5$ $t = 4.29$	6
4	upstream moving wall equiv. to downstr. moving separation turbulent case	steady, modified WJ flow	$u_e = 1 - 0.833x$ $x < x_I$ $u_e = 1 - 0.833x_I$ $x > x_I$ $u_w = -0.166$ $x_I = 0.945x_1$ $x_1 = 0.21$ $Re = 10^3$	8

Table 1: Presented results

3. **The MRS and the STG point streamlines must be different:** The STG point streamline must approach the separated region perpendicular to it, as branching streamlines at a free STG point are always normal to each other.

4. **The MRS and the ORF point do not coincide:** Coincidence of both points would require a bifurcation of the streamline at this point. This is not possible at 2D fluid motions.

We now make use of the arguments 1 to 4. Furtheron, we may state that

1. the maxima (in η-direction) of the streamlines have to be behind the MRS point because in front of the MRS point always upward (positive) v-velocities exist and

2. the line connecting the minima of the u-velocity component approaches the separated flow region continuously, see Fig. 5c.

As a consequence the MRS point is not a complete description of the separation over a downstream moving wall or an upstream moving separation point, respectively. Moreover, three different points in streamwise direction have to be distinguished (Fig. 5b):

- Moore-Rott-Sears point (MRS): First point where u and $\frac{\partial u}{\partial y}$ do vanish.
- Onset of Reverse Flow (ORF): Most upstream point of the separated region.
- Stagnation point (STG): Point where the velocity components u and v do vanish.

The picture Fig. 5b agrees with the velocity profiles of the boundary layers given in Fig. 3. The continuity and the momentum equations are satisfied. This new model holds for laminar as well as for turbulent flows. The mean differences are that the turbulent boundary layer is much thicker as at the laminar case. The separation occurs later in time and in location.

Calculated Results

Calculations with original and modified laminar and turbulent WJ flows were carried out to confirm the previous statements. The transformed locally and temporarily linear retarded flow was modified in such a way that at the end of the computational area the velocity gradient was set to zero in the remaining flowfield, see Tab. 1. This resulted in a boundary layer flow with a separation bubble. By retaining the diffusive term in the boundary layer equations[18] a stable solution for the whole bubble could be achieved. The laminar results agree qualitatively good with the results of O. Inoue[21]. Inoue also has used reduced Navier-Stokes equations and alike boundary conditions. Qualitatively the results from unsteady calculations comply with those from steady calculations with downstream moving wall. Fig. 6 is such a streamline picture for the turbulent case calculated in the wall fixed coordinate system (unsteady). In Fig. 6a this result is presented in in a separation point fixed, in Fig. 6b in a wall fixed coordinate system. As expected, the MRS point is clearly located in front of the separated region starting from the ORF point (Fig. 6a). A closed bubble as the result of the calculation, see also O. Inoue[21], shows that there is only one STG point underneath the separation bubble. Another point with diminishing velocity components is in the center of the separation region.

In the wall fixed coordinate system (Fig. 6b) backflow components are visible near the wall before the sepa-

ration starts.

Downstream Moving Separation Point

General

When the downstream moving wall decelerates the separation moves ahead. The STG, the ORF and the MRS point move towards the wall and coincide there, when the wall velocity vanishes. The definitions of the separation according to the present report, Prandtl's criterion and the MRS criterion become identical. However, if the wall velocity is further increased upstream the description of Prandtl will fail again. The separation moves further ahead. In unsteady flow this corresponds to a separation moving downstream.

For the streamline picture it has been proposed previously that there still exist a STG point and a MRS point in the flow. In contradiction to this picture it is suggested[1] that no STG point and no MRS point is available in order to identify separation.

Published Streamline Pictures

Streamline pictures with STG and MRS point, Fig. 8a, may be found e.g. at W. R. Sears, D. P. Telionis[24] and D. T. Tsahalis[18]. The assumption there is that the STG, the ORF and the MRS point fall together. When the u-velocity profiles pass the zero value they should have a plateau at the MRS point ($u = 0, \frac{\partial u}{\partial y} = 0$), which coincides, as said above, with the STG point. It allows the change from positive to negative velocity at vanishing velocity gradient. The development of a plateau at the u-profiles means an acceleration of the flow near the wall. This is not justified in a region where, because of the validity of the boundary layer equations, the pressure through the boundary layer is nearly constant. Suitable v-profiles of the velocity, which have not been found in the literature, must show several direction changes to comply with the assumed streamlines. Such streamline pattern were not found in any published calculation. Experimental results of moving flat plate boundary layers to verify the streamlines also have not been found. There are only results avaible for rotating circular cylinders[8, 23]. Those results, however, can not be taken for our problem because of the large slope and the curvature of the body contour at the location of separation.

Suggested New Separation Flow Pattern

Alternatively to D. T. Tsahalis the following flow pattern is suggested[1]: When the wall moves upstream the ORF also moves upstream. There, separation is revealed by a strong, sudden increase of the boundary layer thickness. The STG point moves far ahead, i.e. there is no STG point next to the separation region. Accordingly, the velocity profiles in x-direction and in y-direction contain the same characteristic features as those of a downstream moving wall, Fig. 5c. There is no need for the appearance of plateaus for the u-profiles anymore. The v-profiles look alike those of a downstream moving wall.

For the upstream moving wall the three characteristic points, describing the separation for a downstream moving wall, are not valid anymore, because the MRS- and the STG-point move far upstream as seen before. The suddenly very large growing v-component of the velocity accompanied by a very strong increase of the boundary layer thickness, indicate now the separation, see Fig. 7b. Separation still begins at a relatively sharp defined position downstream of the forward part of the plate but, of course, upstream of the separation position of a fixed or downstream moving wall. Therefore a definition was found[1] to describe in a streamline picture the location of separation unequivocally and reproducibly.

The flow close to the wall moves opposite to the external flow. It changes its direction upstream of the separation and aligns with the external flow. When approaching the separation all streamlines that come from upstream first are curved outward. Further downstream they align with the main flow. That means, that streamlines close to the wall have one point where the u-component changes sign followed by two inflection points. The streamlines of the external boundary layer, going downstream only, show, however, no sign change of the u-component and only one inflection point. A line connecting all inflection points, Fig. 7b, has one characteristic point in which both inflection points coincide and consequently disappear. This point belongs to a streamline which can be defined as the separation streamline. The most forward point of it gives the **Onset of Reverse Flow** for the defined separation region (ORF). (For a downstream moving wall the same holds. In this case it becomes the STG point, Fig. 5b). This definition for the separation line is applicable to all flows above moderate curved surfaces, for accelerated and for decelerated flows, for down- and for upstream moving walls and holds as mentioned here for turbulent flows as well.

Proposal For A New Definition Of Unsteady Separation: The separation streamline is the first streamline within the boundary layer without inflection point (Zero Inflection Point).

Calculated Results

The calculation procedure for upstream and downstream moving wall is the same apart from the different wall velocity boundary conditions. The existence of a plateau of the u-velocity component can not be observed, as expected. Streamlines and velocity profiles correspond to the description given before. Fig. 8a and 8b presents such a calculation for the turbulent case, see Tab. 1, in a downstream moving and in a wall fixed coordinate system. Fig. 8b enables the compar-

ison with Fig.7b, no MRS and no STG point is near separation. Fig. 8a, the same result presented in a wall fixed coordinate system, shows the reason: As in the steady case the separation is characterized by a semi-bubble. Its region is limited by the wall and by the separation line.

Experiments: Dynamic Stall At A Pitching NACA 0012 Airfoil

Facility and Model Description

All experiments were carried out in one of the low-speed wind-tunnels of the Technische Universität München. It is a closed-return facility; the nozzle diameter is 1.5 m, the length of the open test section is 3 m. Maximum usable velocity is 55 m/s. Turbulence intensity is known to be under 0.3 - 0.4% over the speed range of interest.

The tunnel is equipped with a data acquisiton system, a probe traversing, a support and a control system all based on a personal computer. Online data transfer and communication with a second computer system, a CONVEX C1 and several work-stations, are required for data storing, reduction and processing by statistical means realizing therefore a complete automatic process of flowfield measurements.

In the dynamic stall tests a carbon fibre model of a NACA 0012 pitching about the quarter-chord axis is used to investigate unsteady separation. To enable a sinusoidal dynamic stall motion a eccentric disk drives a parallel guided rod. Large end plates simulate a quasi two-dimensional flow in the mid section.

Hot-wire Anemometry

Hot-wire anemometry is used to measure the magnitude and the associated direction of the time-dependent velocity vector. The hot-wire probe is operated by a DISA C three-channel constant-temperature anemometer system.

The probe used for this dynamic stall experiment is a new developed cross-wire probe with two additional wires to measure both streamwise and reverse flow, Fig. 9a. The probe axis is mounted normal to the mean flow direction and has, therefore, a very thin probe body and strong outward curved prongs. The measuring volume is about 2 mm. One of the two additional wires is operated as a third hot-wire, the other wire is also heated and hold at a constant temperature. This wire is strongly bended and mounted very close to the third one, Fig. 9a. The forced convection due to the fourth wire causes a significant change in the output signal of the third wire to decide whether streamwise or reverse flow is present. The probe works for all used velocities from -40 m/s to +40 m/s in a yaw angle range from -40 deg to +40 deg.

To calibrate the hot-wire probe a computer-aided fully automated procedure is developed based on a velocity and flow-angle dependent, temperature corrected method.

In order to measure the whole velocitiy range with high accuracy it is necessary to calibrate the new probe in particular for the very low velocity range. Therefore, in addition to the wind-tunnel calibration method an in situ swinging arm calibration method is developed for this range, Fig. 9b. The probe is mounted for discret angles (yaw-angles) on the swinging arm. For every phase-angle of the swinging arm the probe velocity can be calculated. Therefore for each yaw-angle all velocities between -2 m/s and $+2$ m/s are calibrated with one record of a timeseries, only.

Thus a streamwise and a reverse flow calibration grid, each composed of a wind tunnel and an in situ swinging arm calibration grid, are obtained. The resolution of each grid is very fine in the low velocity range (in situ swinging arm calibration) and becomes more coarse for the higher velocities (wind tunnel calibration). In order to select the streamwise or reverse flow corresponding look-up table the two additional wires produce a decision signal quantified as a difference between the output voltages.

For the dynamic stall experiment a mean angle of attack of 10 deg and a amplitude of $+/-10$ deg is chosen. A trigger signal gives the connection between the phase angle and the time series. The pitching frequency of the profile is 2 Hz at a velocity of 12.5 m/s. This leads to a reduced frequency of $k = 0.3$. With a wing chord of 0.3 m a Reynolds number of 2.5×10^5 is obtained.

The measurement plane, Fig. 9c, containes 15 points in chord direction and 12 points perpendicular to it leading to 180 measure points. The sampling frequency for each channel is set to 600 Hz. For each grid point 100 amplitudes of the phase angle are measured. This leads to a sampling time of 50 sec and for 6 channels (4 wires, trigger and temperature) to 180.000 samples at each grid point.

Results and Discussion

Results are shown in Fig. 10 for the phase angles 30, 35, 38, 40, 44 and 48%. (Phase angle means here the actual time beginning with the minimum angle of attack devided by the time for one pitching periode. The NACA 0012 profile is mapped on the lower focal plane in the pictures.) A region with reverse flow components is marching upstream at increasing phase angle starting at the tailing edge at a phase angle of about 21%. This region doesn't show the behavior of a separation, the boundary layer thickness doesn't increase very much. The lift rise remains high.

For the tested Reynolds number and reduced frequency the onset of the dynamic stall vortex is orginated in a

small region of reverse flow comming upstream. When the upstream movement of this reverse flow region becomes slower than the reverse flow velocity components, the onset of the dynamic stall vortex occurs. This happens at the leading part of the profile at a phase angle of 40% and is similar to the unsteady separation as explained in section 3 of this paper. This vortex accelerates the external flow, the flow in the rear part of the profile reattaches and the lift increases further. The vortex grows, looses energy and finally bursts at a phase angle higher then the maximum angle of attack. The lift now breakes down.

With further increasing phase angle, downstroke motion, the bursted vortex disappears and then the flow reattaches uniformely beginning at the leading edge of the profile. Fig. 11 shows this behaviour in the form of instanteanious streamlines for the phase angles 50, 60, 70, 75, 80 and 85%. The boundary layer thickness decreases at every chord position. No STG or MRS point can be identified as mentioned in section 4 of this paper. The fully reattached flow is achieved at a phase angle of about 90%.

Together with the unsteady boundary layer separation calculations perhaps a better look into the dynamic stall phenomena will be found.

Conclusion

The unsteady separation process for boundary layers follows the same pattern as it has been suggested for laminar flows in ref.1. It enables a better understanding and interpretation of effects like the onset of the dynamic stall vortex at a pitching airfoil.

Instead of using the MRS-point as the criterion for unsteady two-dimensional flow separation the following definition which has been suggested for laminar flow is also proposed for turbulent flow: **The separation line is the first streamline within the boundary layer without inflection point.**

- For an upstream moving separation point the previously published flow patterns should be slightly modified. They may be refined by including in addition to the MRS-point two other points, namely the **O**nset of **R**everse **F**low point (ORF) and the **St**agnation point (STG).
- For a downstream moving separation point the same flow pattern as in ref.1 is suggested: The separation streamline is the first streamline without inflection point (Zero Inflection Point). The most upstream point of that line, namely the ORF point, is here the definition point. No MRS- and no STG-point exist near the separation.

Unsteady flowfield measurements with a new developped four-wire probe at a pitching NACA 0012 airfoil in dynamic stall motion show that the onset of the Dynamic Stall Vortex and the reatachment are boundary layer driven effects.

References

[1] H. Ranke and B. Laschka. A new look into two-dimensional unsteady separation. AIAA Journal (in reviewing process: Log. No.: J21193) – also avaible as report FLM–93/16, Lehrstuhl für Fluidmechanik, Technische Universität München.

[2] B. Laschka. Unsteady flows - Fundamentals and applications. In *AGARD CP-386 Conference Proceedings*, pages 1.1–1.21, 1985.

[3] J. C. WilliamsIII and W. D. Johnson. Note on unsteady boundary-layer separation. *AIAA Journal*, 12(10):pp.1427–1429, October 1974.

[4] F. K. Moore. On the separation of the unsteady laminar boundary layer. Boundary Layer Research, edited by H. G. Görtler, Springer Verlag, Berlin, 1958.

[5] N. Rott. Unsteady viscous flow in the vicinity of a stagnation point. *Quarterly of Applied Mathematics*, 13(1):pp.444–451, 1955.

[6] W. R. Sears. Some recent developements in airfoil theory. *Journal of the Aeronautical Sciences*, 23(5):pp.490–499, May 1956.

[7] J. C. WilliamsIII. Incompressible boundary-layer separation. *Annual Reviews of Fluid Mechanics*, 9:pp.113–144, 1977.

[8] C. A. Koromilas and D. P. Telionis. Unsteady laminar separation : An experimental study. *J.Fluid.Mech.*, 97(2):pp.347–384, 1980.

[9] L. L. Dommelen and S. F. Shen. An unsteady interactive separation process. *AIAA Journal*, 21(3):p.5, March 1983.

[10] R.A. McD. Galbraith, M.W. Gracey, and R. Gilmour. *Collected Data for Tests on a NACA 0012 Aerofoil.* University of Glasgow, Department of Aerospace Engineering, Report 9208, Feb. 1992.

[11] L.W. Carr, K.W. McAlister, and W.J. McCroskey. *Analysis of the Development of Dynamic Stall Based on Oscillating Airfoil Experiments*, NASA-TN-8382 edition, Jan. 1977.

[12] H. Schlichting. *Grenzschicht-Theorie.* Verlag G. Braun; Karlsruhe, 1965.

[13] A.D. Young. *Boundary Layers.* BSP Professional Books, London, 1989.

[14] T. Cebeci. Calculation of unsteady two-dimensional laminar and turbulent boundary layers with fluctuations in external velocity. In *Proc.R.Soc.Lond.*, page 14, 1977.

[15] W. J. McCroskey and J. J. Philippe. Unsteady viscous flow on oscillating airfoils. *AIAA*, 13(1):p.9, January 1975.

[16] B.S. Baldwin and H. Lomax. Thin layer approximation and algebraic model for separated turbulent flows. In *AIAA 16th Aerospace Meeting.* Huntsville, 1978.

[17] W. Rodi. *Introduction to the Modelling of Turbulence.* von Karman Institute for Fluid Dynamics, Brüssel, 1985.

[18] D. T. Tsahalis. Laminar boundary-layer separation from an upstream-moving wall. *AIAA Journal*, 15(4), 1977.

[19] J. C. WilliamsIII and T. J. Wang. Semisimilar solutions of the unsteady compressible laminar boundary-layer equations. *AIAA Journal*, 23(2):pp.228–233, February 1985.

[20] D. P. Telionis and M. J. Werle. Boundary-layer separation from downstream moving boundaries. *Transactions ASME Journal of Applied Mechanics*, E 40:pp.369–374, Juni 1973.

[21] O. Inoue. MRS criterion for flow separation over moving walls. *AIAA Journal*, 19(9):pp.1108–1111, 1981.

[22] A. Leder. *Abgelöste Strömungen, Physikalisch Grundlagen.* Vieweg, 1992.

[23] G. R. Ludwig. An experimental investigation of laminar separation from a moving wall. In *AIAA Paper No. 64-6*, page 12, January 20-22 1964.

[24] W. R. Sears and D. P. Telionis. Boundary-layer separation in unsteady flow. *SIAM Journal of Applied Mathematics*, 28(1):pp.215–235, 1975.

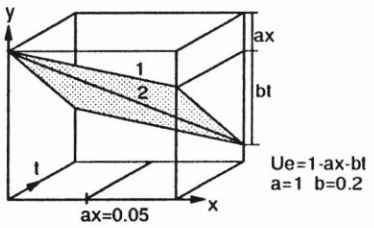

a) WJ–external velocity U_e

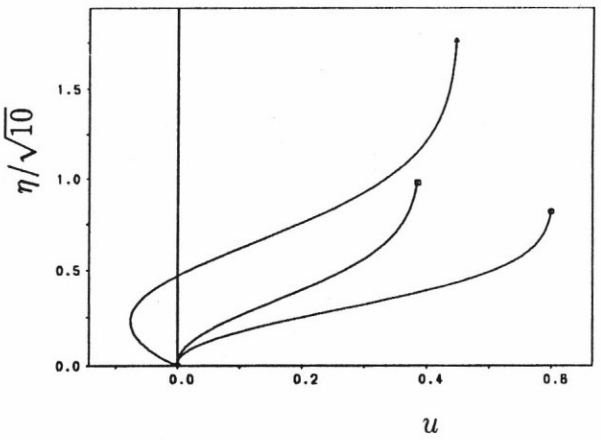

b) □ steady calculation, pressure gradient corresponding Fig. 1a gradient 1; $x_1 = 0.384$
○ quasisteady calculation, pressure gradient corresponding Fig. 1a gradient 2; $x_1 = 0.599$
△ unsteady calculation; $x_1 = 0.05, t = 2.52$

Figure 1: Comparison: Steady, quasisteady and unsteady velocity profiles for a Williams-Johnson flow

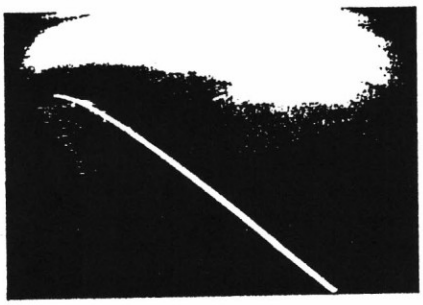

(a) NACA 0012 at $\alpha = 20°$
steady case

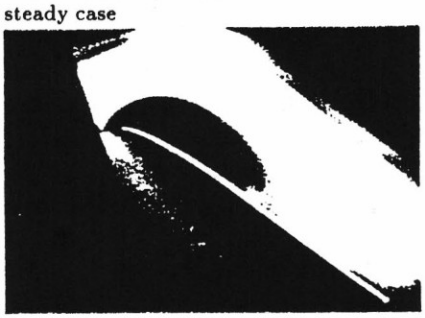

(b) NACA 0012 at $\alpha = 20°$
$k = 0.3$, upstroke motion

Figure 2: Laser light sheet visualisation at a NACA 0012 airfoil

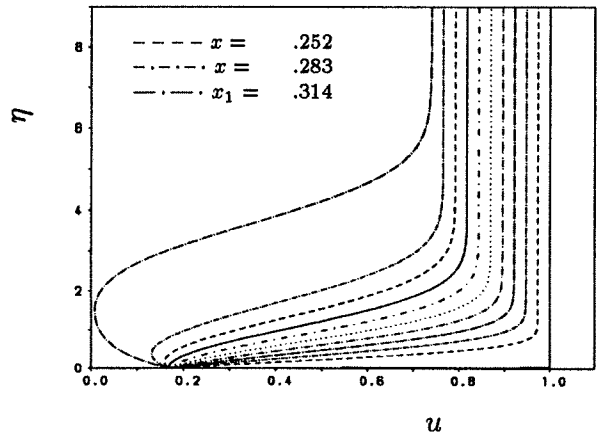

(a) u vs. η

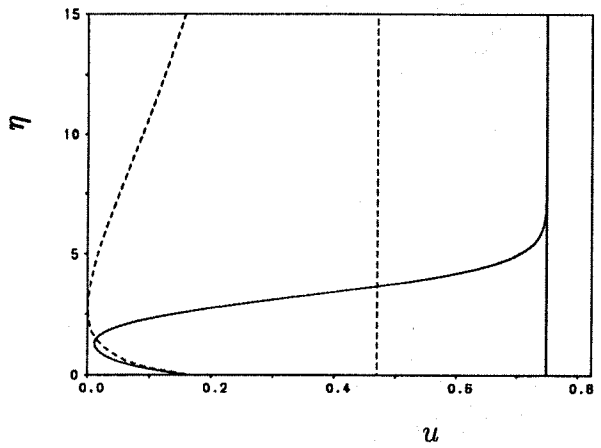

(b) ——— lam.: $x = 0.31$, $u_1 = 0.75$
- - - - turb.: $x = 0.64$, $u_1 = 0.47$

Figure 3: u-Velocity profiles, steady WJ flow

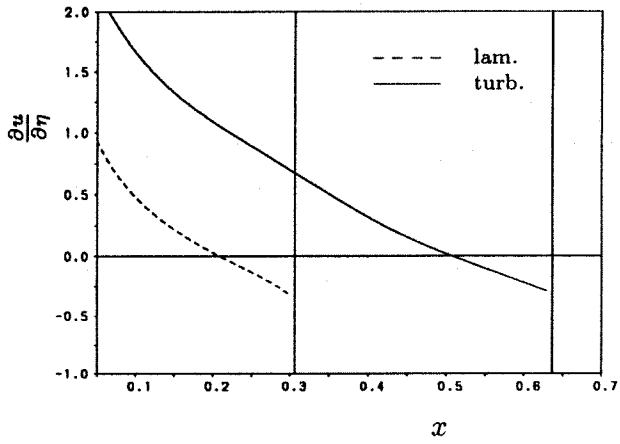

(a) wall velocity gradient (wall shear stress)

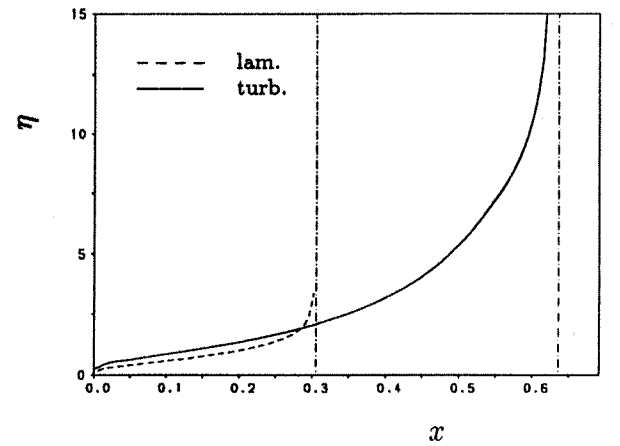

(b) displacement Thickness

Figure 4: Boundary layer quantities, steady WJ flow

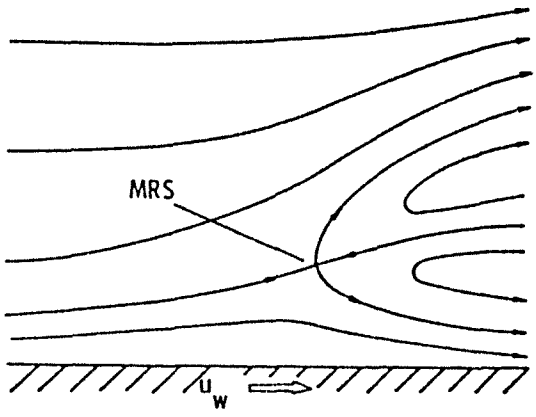

(a) Streamline pattern of D. P. Telionis and M. J. Werle[20]

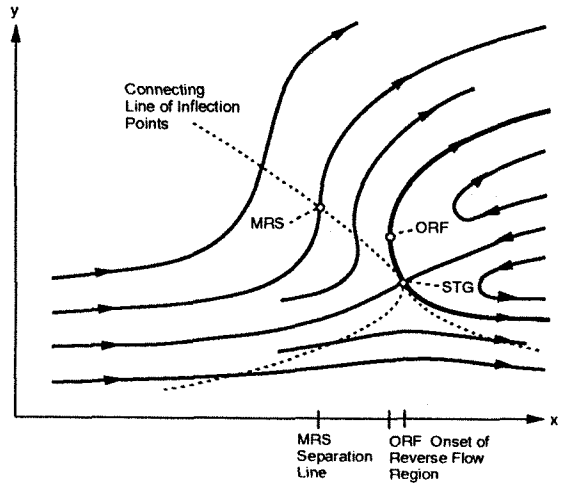

(b) New streamline pattern from H. Ranke and B. Laschka[1]

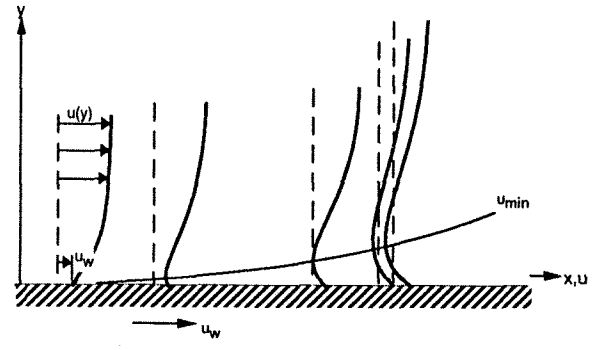

(c) u-Profiles

Figure 5: Downstream moving wall – previous (a) and new (b) streamline picture and u-velocity profiles (c)

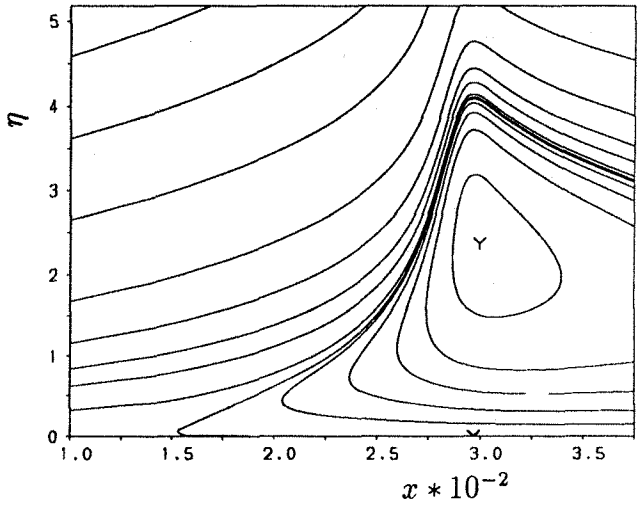

(a) Y $u = 0$; $v = 0$ at the center of the bubble boundary conditions for the calculation see Tab. 1 unsteady result presented in the wall fixed coordinate system

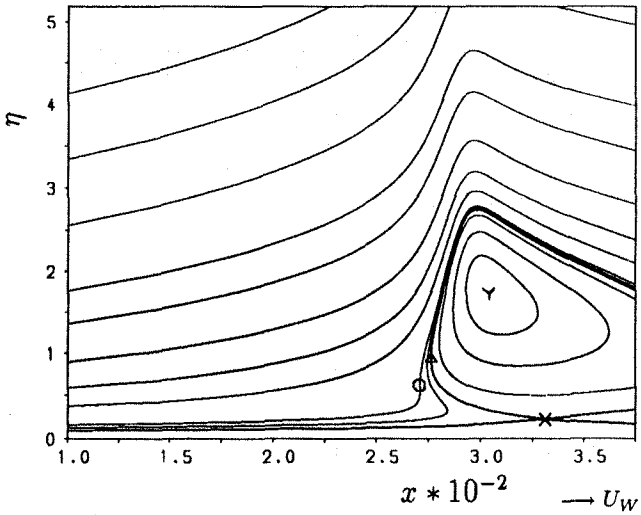

(b) ○ MRS point
△ ORF point
X STG point
Y $u = 0$; $v = 0$ at the center of the bubble boundary conditions for the calculation see Tab. 1 unsteady result presented in a upstream moving coordinate system

Figure 6: Calculated streamline picture: Separation bubble for an upstream moving separation point

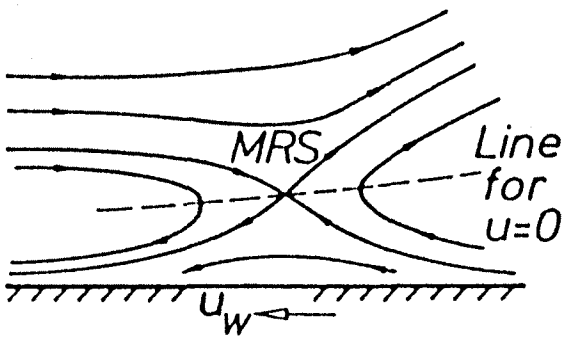

(a) Streamline pattern of D. T. Tsahalis[18]

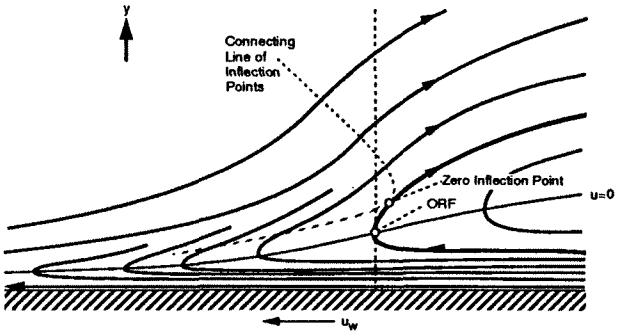

(b) New streamline pattern from H. Ranke and B. Laschka[1]

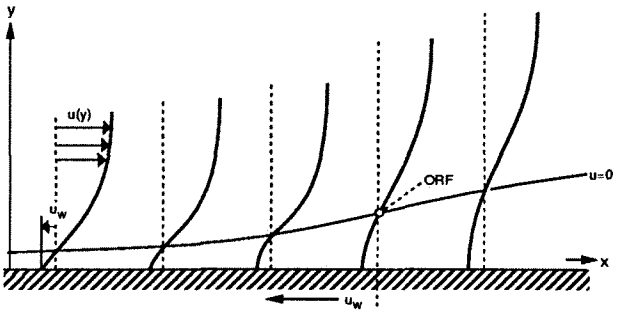

(c) u-Profiles

Figure 7: Upstream moving wall – previous (a) and new (b) streamline picture and u-velocity profiles(c)

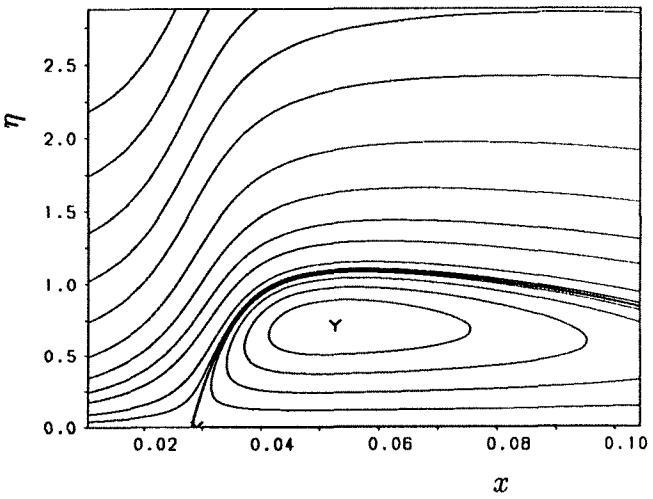

(a) Y $u = 0$; $v = 0$ at the center of the bubble boundary conditions for the calculation see Tab. 1 steady result presented in a wall fixed coordinate system

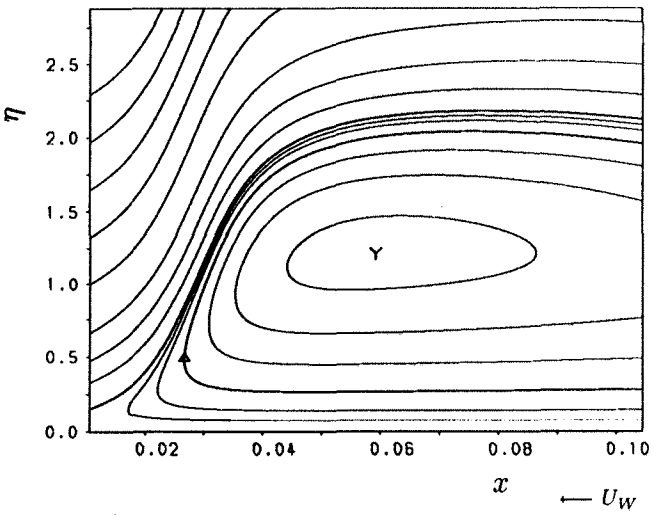

(b) △ ORF point
Y $u = 0$; $v = 0$ at the center of the bubble boundary conditions for the calculation see Tab. 1 steady result presented in the downstream moving coordinate system

Figure 8: Calculated streamline picture: Separation bubble for an upstream moving wall

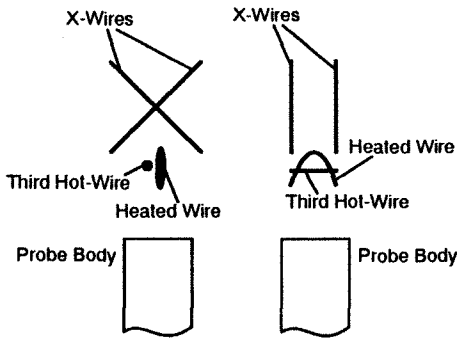

(a) new four-wire probe

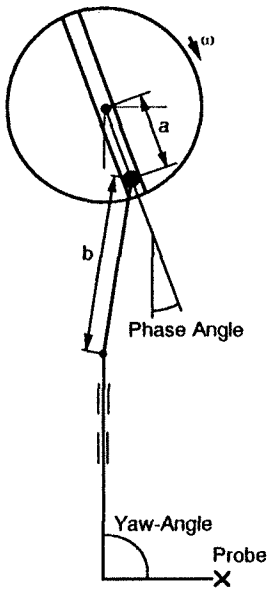

(b) in-situ swinging arm calibration

$$w = -\omega a \sin\Theta * \left(1 + \frac{\cos\Theta}{(b^2/a^2 - \sin^2\Theta)^{0.5}}\right)$$

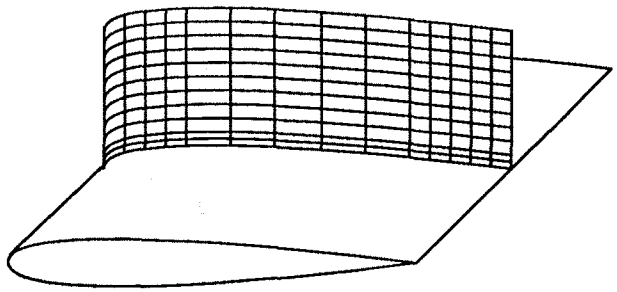

(c) measurement plane at the pitching NACA 0012 airfoil

Figure 9: Pitching NACA 0012 Airfoil: Probe, Calibration Method and Measurement Plane

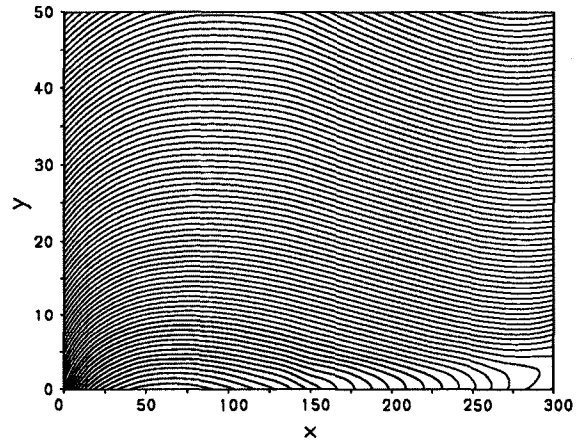

(a) $t/T = 0.30$

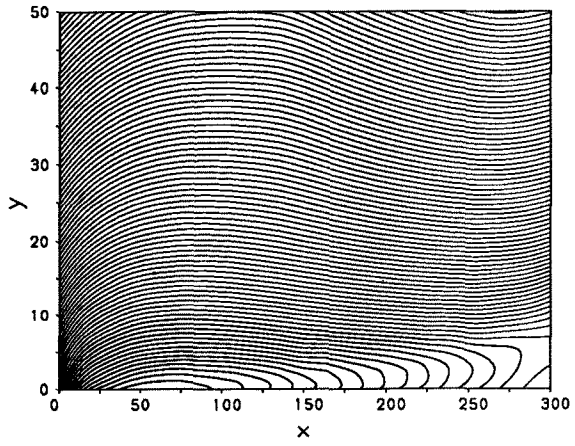

(b) $t/T = 0.35$

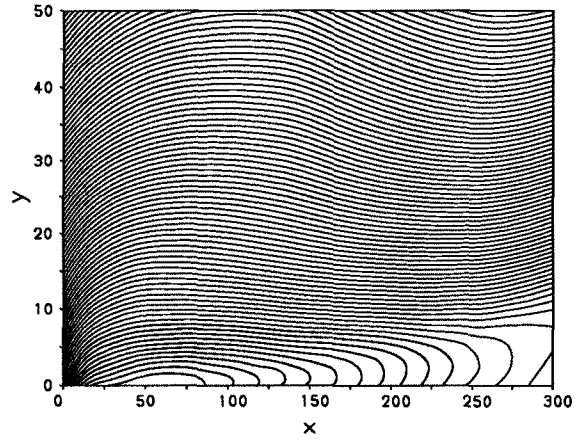

(c) $t/T = 0.38$

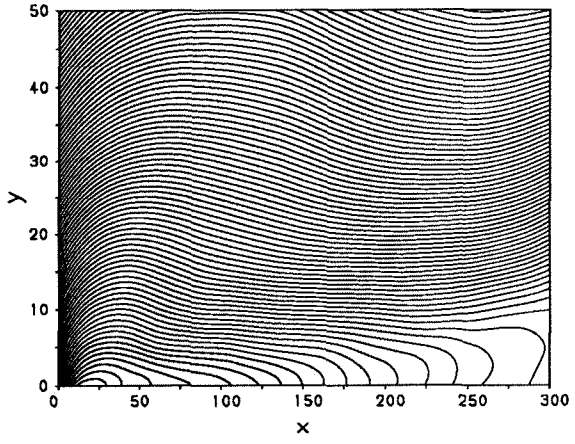

(d) $t/T = 0.40$

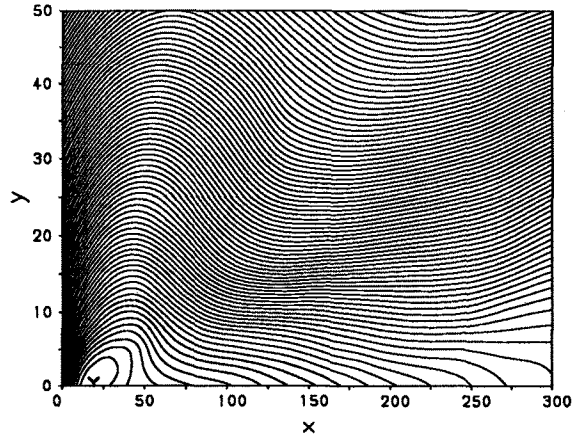

(e) $t/T = 0.44$

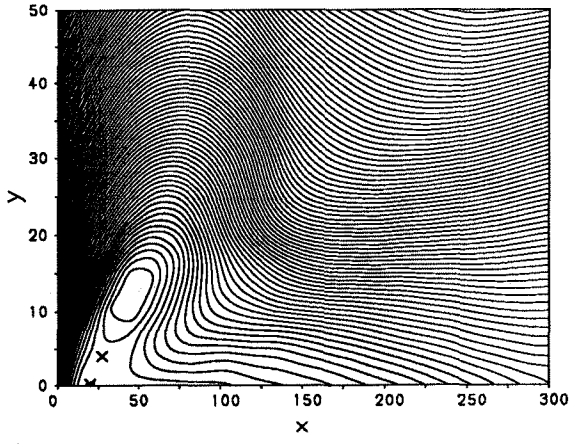

(f) $t/T = 0.48$

Figure 10: Pitching NACA 0012 Airfoil: Streamlines at Upstroke Motion

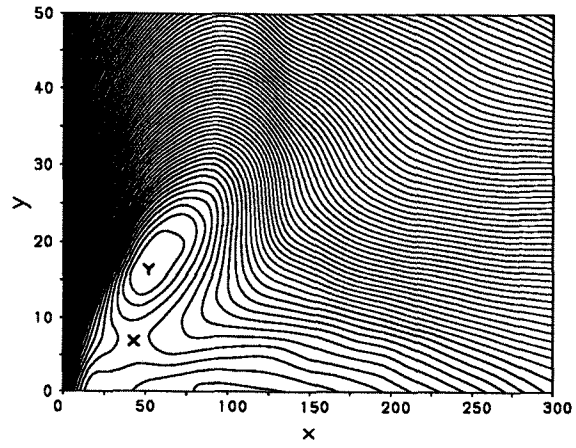

(a) $t/T = 0.50$

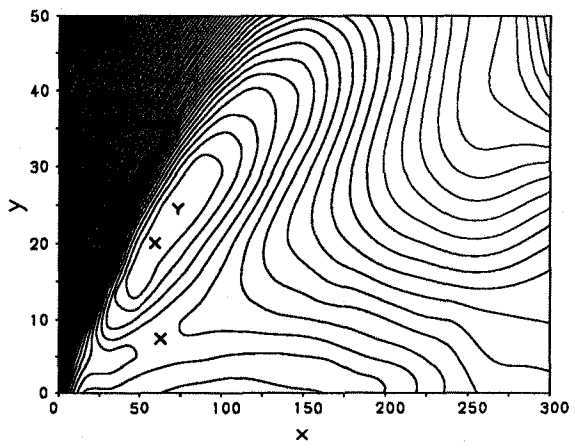

(b) $t/T = 0.60$

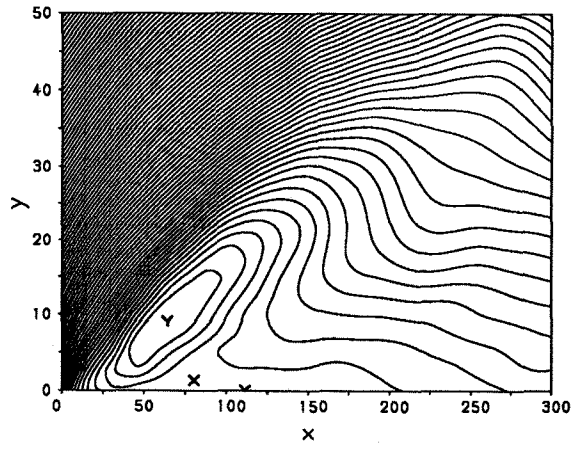

(c) $t/T = 0.70$

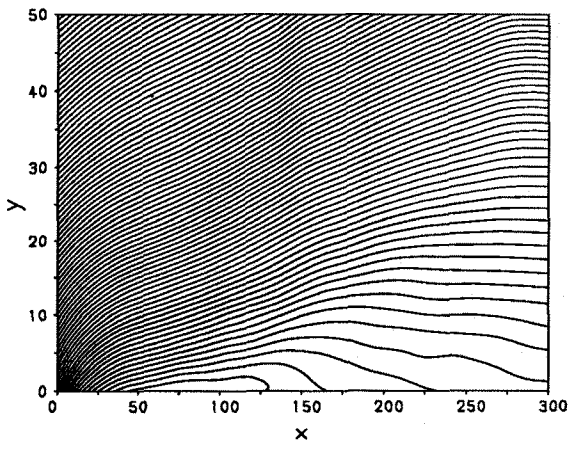

(d) $t/T = 0.75$

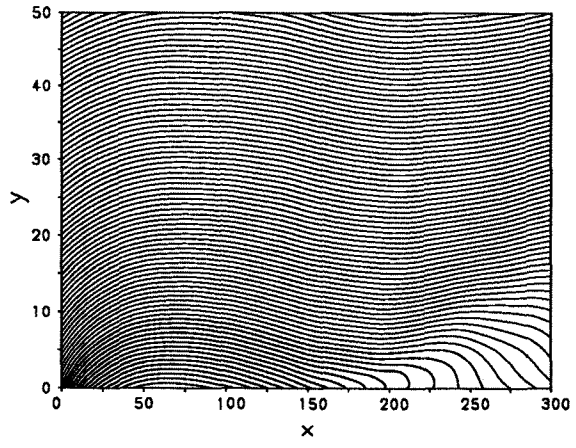

(e) $t/T = 0.80$

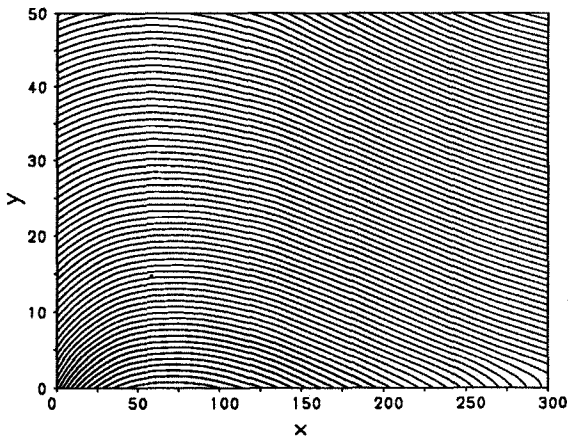

(f) $t/T = 0.85$

Figure 11: Pitching NACA 0012 Airfoil: Streamlines at Downstroke Motion